NeuroImage 234 (2021) 117957

Contents lists available at ScienceDirect

NeuroImage

journal homepage: www.elsevier.com/locate/neuroimage

# Feedforward and feedback pathways of nociceptive and tactile processing in human somatosensory system: A study of dynamic causal modeling of fMRI data

Yingchao Song[a], Qian Su[b], Qingqing Yang[a], Rui Zhao[a,c], Guotao Yin[b], Wen Qin[d], Gian Domenico Iannetti[e,f], Chunshui Yu[d,g], Meng Liang[a,*]

[a] School of Medical Imaging and Tianjin Key Laboratory of Functional Imaging, Tianjin Medical University, Tianjin, China
[b] Department of Molecular Imaging and Nuclear Medicine, Tianjin Medical University Cancer Institute and Hospital, National Clinical Research Center for Cancer, Tianjin Key Laboratory of Cancer Prevention and Therapy, Tianjin's Clinical Research Center for China, Tianjin, China
[c] Department of Orthopedics Surgery, Tianjin Medical University General Hospital, Tianjin, China
[d] Department of Radiology and Tianjin Key Laboratory of Functional Imaging, Tianjin Medical University General Hospital, Tianjin, China
[e] Neuroscience and Behaviour Laboratory, Italian Institute of Technology, Rome, Italy
[f] Department of Neuroscience, Physiology and Pharmacology, University College London, London, United Kingdom
[g] Chinese Academy of Sciences (CAS) Center for Excellence in Brain Science and Intelligence Technology, Chinese Academy of Sciences, Shanghai, China

ARTICLE INFO

*Keywords:*
Somatosensory system
Nociceptive processing
Parallel processing
Feedback modulation
Dynamic causal modeling

ABSTRACT

Nociceptive and tactile information is processed in the somatosensory system via reciprocal (i.e., feedforward and feedback) projections between the thalamus, the primary (S1) and secondary (S2) somatosensory cortices. The exact hierarchy of nociceptive and tactile information processing within this 'thalamus-S1-S2' network and whether the processing hierarchy differs between the two somatosensory submodalities remains unclear. In particular, two questions related to the ascending and descending pathways have not been addressed. For the ascending pathways, whether tactile or nociceptive information is processed in parallel (i.e., 'thalamus-S1′ and 'thalamus-S2′) or in serial (i.e., 'thalamus-S1-S2′) remains controversial. For the descending pathways, how corticothalamic feedback regulates nociceptive and tactile processing also remains elusive. Here, we aimed to investigate the hierarchical organization for the processing of nociceptive and tactile information in the 'thalamus-S1-S2' network using dynamic causal modeling (DCM) combined with high-temporal-resolution fMRI. We found that, for both nociceptive and tactile information processing, both S1 and S2 received inputs from thalamus, indicating a parallel structure of ascending pathways for nociceptive and tactile information processing. Furthermore, we observed distinct corticothalamic feedback regulations from S1 and S2, showing that S1 generally exerts inhibitory feedback regulation independent of external stimulation whereas S2 provides additional inhibition to the thalamic activity during nociceptive and tactile information processing in humans. These findings revealed that nociceptive and tactile information processing have similar hierarchical organization within the somatosensory system in the human brain.

## 1. Introduction

Nociceptive and tactile signals are transmitted from peripheral pathways to the somatosensory cortices via thalamus which is an important relay station for sensory information transmission (Forss and Jousmaki, 1998; Treede et al., 1999). The information transfer between the thalamus and the somatosensory cortices, mainly including the primary (S1) and the secondary (S2) somatosensory cortices, is most likely reciprocal (Alitto and Usrey, 2015). However, it remains undetermined how somatosensory information is transmitted from the thalamus to S1 and S2 (i.e., the exact ascending pathway) and how these cortical areas modulate the thalamic activity (i.e., the exact descending pathway). Importantly, it also remains unclear whether the ascending and descending pathways are the same or different for nociceptive and tactile information transmission within this 'thalamus-S1-S2' network. This is particularly important for understanding whether nociceptive-specific information, compared with tactile information, might be encoded in the connectivity pattern of the somatosensory system (Hu and Iannetti, 2016; Liang et al., 2013, 2019; Wager et al., 2013; Su et al., 2019).

* Corresponding author. School of Medical Imaging, Tianjin Medical University, 1 Guangdong Road, Hexi District, Tianjin, 300203, China.
*E-mail address:* liangmeng@tmu.edu.cn (M. Liang).

https://doi.org/10.1016/j.neuroimage.2021.117957
Received 27 June 2020; Received in revised form 7 March 2021; Accepted 9 March 2021
Available online 17 March 2021
1053-8119/

Regarding the ascending pathways in the 'thalamus-S1-S2' somatosensory system, compelling evidence from electrophysiological and anatomical tracing studies in animals has shown that both S1 and S2 receive direct projections from multiple thalamic nuclei such as the ventral posterior nucleus (VP), the ventral posterior inferior nucleus (VPI), and the centrolateral nucleus (CL) (Friedman and Murray, 1986; Jones, 1998; Krubitzer and Kaas, 1992) and that there are extensive corticocortical projections between S1 and S2 (Burton and Carlson, 1986; Friedman et al., 1980; Pons and Kaas, 1986). For nociceptive processing, several studies have suggested that nociceptive information is transmitted from the thalamus to S1 and to S2 via segregated thalamocortical pathways (i.e., a parallel processing in S1 and S2) in both lower and higher primates (Gingold et al., 1991; Shi et al., 1993; Stevens et al., 1993). Consistent with the evidence from animals, current evidence from human studies, except one (Khoshnejad et al., 2014), also supports that nociceptive information is transmitted from the thalamus to the S1 and the S2 in parallel. For example, using source reconstruction of magnetoencephalographic (MEG) responses to nociceptive stimuli in humans, Ploner et al. observed that the responses hypothesized to originate from S1 and S2 had similar onset times (~130 ms) and that the S2 activity was not causally influenced by the S1 activity during nociceptive stimulation (Ploner et al., 1999, 2009). Using dynamic causal modeling (DCM) of fMRI responses to nociceptive stimuli, we found that nociceptive somatosensory inputs modulated in parallel the connectivity from the thalamus to S1 and the connectivity from the thalamus to S2 (Liang et al., 2011). For tactile processing, however, there are currently two competing hypotheses from both animal and human studies: 'serial pathway' vs. 'parallel pathway'. The 'serial pathway' hypothesis proposes that somatosensory signals are projected from the thalamus to S1 and then from S1 to S2; in other words, there is no direct transmission of tactile information from the thalamus to S2. In contrast, the 'parallel pathway' hypothesis proposes that tactile information is transmitted from the thalamus directly to both S1 and S2. In animal studies, most evidence supports that tactile information is processed in parallel in lower primates (Garraghty et al., 1991; Turman et al., 1992) but is processed serially from S1 to S2 in higher primates (Allison et al., 1989a, 1989b; Hari et al., 1993; Inui et al., 2004; Mima et al., 1998; Ploner et al., 2009; Pons et al., 1992; Schnitzler et al., 1999), which has been interpreted as a result of an evolutionary shift from parallel processing to serial processing (Mountcastle, 2005). Indeed, some human studies also showed results suggesting serial processing for tactile information, consistent with such evolutionary shift. However, evidence supporting parallel processing of tactile information in S1 and S2 of higher primates (Rowe et al., 1996; Zhang et al., 1996) and humans also exist (Karhu and Tesche, 1999). In particular, using DCM combined with Bayesian model selection (BMS) (Stephan et al., 2009) based on fMRI responses to tactile stimuli in humans, two previous studies reported that their data were in favor of the model representing a sequential information transmission from S1 to S2 (Kalberlah et al., 2013; Khoshnejad et al., 2014), whereas opposite findings were also observed using the same technique, that is, the winning model corresponded to a parallel information processing in both S1 and S2 during tactile stimulation (Chung et al., 2014; Liang et al., 2011). Therefore, whether tactile information is processed in parallel or in serial in S1 and S2 in humans still remains a matter of debate (Iwamura, 1998; Rowe et al., 1996).

Most of the evidence based on human studies was established using DCM, an effective connectivity (EC) analysis method for making inferences about how neural activities in one brain region exert influence on neural activities in another region ( Friston et al., 2003). Although DCM is one of the most popular and theoretically advanced methods for EC analysis, these previous studies may suffer from several limitations which may affect the reliability of the results. First, temporal resolution of the fMRI signals is a key factor that affects the estimation of the EC parameters. The causal relationship inferred by DCM is determined using a dynamic function which, by definition, is sensitive to the temporal resolution of fMRI signals ( Friston et al., 2003). However, the highest sampling rate used in these previous studies were 0.5 Hz (i.e., repetition time [TR] = 2 s). With the rapid development of MR acquisition techniques, especially multiband imaging (Moeller et al., 2010), sub-second TR is becoming increasingly popular which may lend DCM better ability to extract causal information from fMRI data. Second, it has been proved that the accuracy of the predefined model structure (e.g., which brain regions or connections are included in the DCM) may also affect the accuracy of the estimated EC parameters (Stephan et al., 2010). A number of animal studies suggested that the thalamus not only sends neural signals to cortical areas but also receives modulatory feedback from cortical areas (Auer, 1956; Jones and Powell, 1968, 1970; Liao et al., 2010; Stratford, 1954). Indeed, it has been shown that the corticothalamic feedback projections are much more numerous (about ten times) than thalamocortical projections (Guillery, 1967; Liu et al., 1995). However, none of the previous studies included the feedback pathways in the DCM. Therefore, it is important to include the feedback pathways in the DCM when investigating the information transfer within the somatosensory system. Moreover, small sample size is also a major limiting factor which obviously undermines the reliability of the results (Button et al., 2013) in these previous studies. Indeed, the largest sample size of these previous studies was 15 subjects. Studies with larger sample sizes are needed to confirm the previous findings. All these limitations make it an open question whether similar or different hierarchical organizations are adopted for nociceptive and tactile information processing within the 'thalamus-S1-S2' network.

Therefore, in the present study, we adopted a more realistic DCM (i.e., including both feedforward and feedback pathways between the thalamus and the S1/S2) combined with high temporal resolution fMRI data (TR = 0.8 s) acquired from a large sample ($n$ = 57 after quality control) to further clarify whether nociceptive and tactile information flows in a similar manner within the somatosensory system. More specifically, we aimed to address the following three questions: (1) whether the cortical processing of nociceptive and tactile information in S1 and S2 are serial or parallel; (2) how somatosensory cortices (i.e., S1 and S2) exert feedback modulation on the thalamus during nociceptive and tactile processing; and (3) whether the hierarchical organization of the 'thalamus-S1-S2' network is different for nociceptive processing than for tactile processing, and thus can serve as a neural coding mechanism for nociception.

## 2. Materials and methods

### 2.1. Participants

Sixty-two healthy volunteers participated in this study (24 males and 38 females, age: 23.9 ± 2.2 years). All subjects were right-handed according to the Chinese edition of the Handedness Inventory (Oldfield, 1971). They did not have any history of neurological or psychiatric disease. Each subject provided an informed consent before participating in the experiment. This study was approved by the Medical Research Ethics Committee of Tianjin Medical University General Hospital.

### 2.2. Experimental design and data acquisition

While lying in the scanner, participants received stimuli of two different sensory modalities, each with two stimulus intensities: nociceptive (low, high) and tactile (low, high) stimuli. Nociceptive stimuli were pulses of radiant heat (5-ms duration) generated by an infrared neodymium yttrium aluminium perovskite (Nd:YAP) laser (wavelength:1.34 $\mu$m; ElEn Group, Italy). Such laser pulses are optimal to selectively elicit painful pinprick sensation (i.e., A$\delta$ inputs) without the contamination by activations of tactile related receptors (i.e., A$\beta$ inputs) (Cruccu et al., 2003; Iannetti et al., 2003). These nociceptive laser stimuli were delivered to the right foot dorsum within the sensory territory

of the superficial peroneal nerve by means of laser pulses. Tactile stimuli were constant current square-wave electrical pulses (2-ms duration; intensity below pain threshold determined in each individual; DS7A, Digitimer Ltd., UK) delivered through a pair of skin electrodes (1-cm inter-electrode distance) over the superficial peroneal nerve of the right foot. During the experiment, subjects were instructed to rate the intensity of every stimulus using a 10-point visual analogue scale (VAS; for nociceptive stimulation, 0 indicates no pain and 10 indicates the most severe pain one can imagine; for tactile stimulation, 0 indicates no sensation and 10 indicates the strongest sensation one can imagine) presented on a screen by pressing the left or the right button using their index or middle finger on a button box. Prior to the scanning, subjects were familiarized with the stimuli and the rating procedure inside the scanner. To account for the inter-subject variability of painful and tactile sensitivity, the physical intensities of nociceptive and tactile stimuli were adjusted for each participant using the following procedure to ensure that all participants perceived laser stimuli as painful and electrical stimuli as non-painful: for each participant, a series of laser and tactile stimuli with different intensities were presented and rated by the participant before the fMRI experiment; laser stimuli of the physical intensities corresponding to a rating of 3 and 6 were used in the formal fMRI experiment as the 'low-intensity' and 'high-intensity' nociceptive stimuli, respectively; similarly, electrical stimuli of the physical intensities corresponding to a rating of 3 and 6 were used as the 'low-intensity' and 'high-intensity' tactile stimuli, respectively. Including stimuli of two physical intensities in the experiment could increase the variability of the perceived stimulus intensity, making it harder for the participants to predict the stimulus intensity, and thus help maintain participants' attention level during the experiment. As the focus of the present study was the differences between the two sensory modalities regardless of stimulus intensity, high and low intensity stimuli of each sensory modality were pooled together to increase the statistical power in the main analyses of the present study (however, the effect of stimulus intensity was examined in a control analysis).

The experiment included two sessions of fMRI data acquisition, with 3 'painful' blocks and 'tactile' blocks in each session (there were 4 trails of each modality in each block), for a total of 48 trials (24 nociceptive trials and 24 tactile trials). Each trial consisted of a stimulation period (~10 s), followed by a rating period (~10 s) with a gap (~2 s) between the onset of the trial and the onset of the stimulation period and a gap (~3 s) between the end of the stimulation period and the beginning of the rating period. During the stimulation period, a single stimulus was delivered at a random time (uniform distribution) and participants are instructed to fixate on a white cross at the center of the screen. During the rating period, subjects were asked to rate the perceived intensity of the stimulus in the same trial using the same 10-point VAS displayed on the screen. To compare the subjective ratings between modalities (nociceptive vs. tactile) and intensities (high vs. low), we first calculated four average ratings for each condition (low-nociceptive, high-nociceptive, low-tactile, high-tactile) in each subject and then these average ratings were compared using a two-way repeated-measure ANOVA. This dataset has been reported in two of our previous studies (Liang et al., 2019; Su et al., 2019), and an illustration of the experimental design can be found in Supplementary Fig. S2b of the previous study (Liang et al., 2019).

Whole-brain fMRI data were acquired using a MAGNETOM Prisma 3T MR scanner (Siemens, Erlangen, Germany) with a 64-channel phase-array head-neck coil. Tight but comfortable foam padding was used to minimize head motion, and earplugs were used to reduce scanner noise. Functional images were acquired with a prototype simultaneous multi-slices gradient echo echo-planar imaging (EPI) sequence (echo time [TE] = 30 ms, TR = 800 ms, field of view [FOV] = 222 × 222 $mm^2$, matrix = 74 × 74, in-plane resolution = 3 × 3 $mm^2$, flip angle [FA] = 54°, slice thickness = 3 mm, gap = 0 mm, number of slices = 48, slice orientation = transversal, bandwidth = 1690 Hz/Pixel, PAT [Parallel Acquisition Technique] mode, slice acceleration factor = 4, phase encoding acceleration factor = 2). A high-resolution 3D T1-wighted structural image was acquired with two inversion contrast magnetization prepared rapid gradient echo sequence (MP2RAGE) (TE = 3.41 ms, TR = 4000 ms, inversion times [TI1/TI2] = 700 ms / 2110 ms, FA1/FA2 = 4°/5°, matrix = 256 × 240, FOV = 256 × 240 $mm^2$, number of slices = 192, in-plane resolution = 1 × 1 $mm^2$, slice thickness = 1 mm, slice orientation = sagittal).

### 2.3. Data pre-processing and activation analyses

Data pre-processing and statistical analysis were performed using MATLAB (Mathworks, Natick, MA, USA) and SPM12 software (Wellcome Trust centre for Neuroimaging, London, UK; http://www.fil.ion.ucl.ac.uk/spm/). Scanned volumes of each subject were realigned to the first volume using a six-parameter (rigid-body) spatial transformation to compensate the motion effect. Two participants with excessive motion artifacts (displacement in any of the three axes greater than 3 mm and rotation around any axis greater than 3°) were excluded from subsequent analyses. The images were co-registered with the subjects' corresponding structural (T1-weighted) images, normalized to the Montreal Neurological Institute (MNI) standard brain and resampled to 3 × 3 × 3 $mm^3$ voxel size. Normalized data were then spatially smoothed (5 mm full width at half maximum [FWHM]) using a Gaussian kernel. Finally, the time series from each voxel were filtered using a high-pass filter with a cut-off period of 128 s to remove low-frequency noise and signal drifts.

We used a general linear model to obtain individual statistical parametric maps with regressors modeling the occurrence of each of the 3 types of events (nociceptive stimuli, tactile stimuli and the rating period) using event-related manner and their corresponding temporal derivatives. Additional regressors were defined using the six head motion parameters and framewise displacement (FD) (Power et al., 2012). Two contrast vectors, one with the regressor of nociceptive stimuli set to 1 and the other with the regressor of tactile stimuli set to 1, were used to identify voxels showing significant responses to nociceptive stimuli and to tactile stimuli, respectively. Individual contrast maps of nociceptive and tactile conditions were used to obtain the group-level nociceptive and tactile activation maps using one-sample t tests. The individual statistical maps were thresholded using $P<0.05$ (uncorrected) whereas group-level statistical maps were corrected using family-wise-error (FWE) method at voxel level ($P<0.05$, corrected) based on Gaussian Random Field (GRF) theory (Nichols and Hayasaka, 2003). Here, we used uncorrected thresholding for individual activation analyses to ensure that the three ROIs (i.e., the thalamus, S1 and S2) required in the subsequent DCM analyses could be identified in most participants (Khoshnejad et al., 2014; Liang et al., 2011).

In order to identify the brain areas responding to both nociceptive and tactile stimuli, a common activation map was generated for each participant by overlapping the activation maps of the two conditions obtained from this participant (Nichols et al., 2005). In this common activation map, the values of the overlapping voxels were taken as the average T values of the two conditions and the values of all other voxels were set to zero. Similarly, a common activation map at the group-level was also generated using the group-level activation maps of the nociceptive and tactile conditions.

### 2.4. ROI definition

Three regions of interest (ROIs) (i.e., the thalamus, S1 and S2, all contralateral to the stimulated side) were defined for each participant in the following steps. 1) Three anatomically defined masks were created using the automated anatomical labeling (AAL) atlas (Tzourio-Mazoyer et al., 2002): the S1 mask was defined as AAL areas 57 (the left postcentral gyrus), 69 (the left paracentral lobule) (Allison et al., 1996) and 67 (the left precuneus) (Omori et al., 2013; Sanchez Panchuelo et al., 2018) and restricted to the medial wall (i.e., the S1 area corresponding to the foot)

as only the right foot was stimulated in the present study (coordinates $x > -33$ mm, $-50$ mm$< y < -27$ mm and $z > 45$ mm); the S2 mask was defined as AAL areas 17 (the left Rolandic_operculum) and 63 (the left supramarginal gyrus) (Beauchamp et al., 2009; Ruben et al., 2001); and the thalamus mask was defined as AAL area 77 (the left thalamus). 2) The group-level peak voxel for each region (i.e., the thalamus, S1 and S2) was identified from the group-level common activation map within the corresponding mask created in step 1. 3) For each participant, the peak voxel of each region was defined from the individual common activation map as the local maximum nearest to the group-level peak voxel within a 10-mm-radius sphere centered at the group-level peak voxel and the corresponding anatomical mask. 4) For each participant, the ROI of each region was finally defined as a 5-mm-radius sphere centered at the identified peak voxel of this participant. If there was no voxels surviving the threshold in the activation map of a particular participant (uncorrected $P<0.05$) in any of the three regions, this participant would be discarded from the subsequent analyses. Specifically, the contralateral thalamus of three participants did not reach this threshold and thus these three participants were excluded from the subsequent DCM analyses. For each of the remaining 57 participants and each ROI, the fMRI time series were extracted by calculating the first eigenvariate from all voxels included in the ROI, adjusted for the F contrast of effects of no-interests to remove the head motion, as implemented in SPM12.

### 2.5. Dynamic causal modeling at individual level

Dynamic Causal Modeling (DCM) is an effective connectivity analysis method for making inferences about causal relationship between neural processes of different brain regions that underlie measured blood-oxygenation-level-dependent (BOLD) fMRI time series ( Friston et al., 2003). The general idea of DCM is to model the neural dynamics driven by one or more external inputs through causal influences among several pre-selected brain regions and then predict the BOLD signals so that the predicted BOLD signals correspond as closely as possible to the observed BOLD time series. Compared with Granger Causality Mapping (Goebel et al., 2003) which is another popular effective connectivity analysis method using temporal precedence of BOLD signals to infer causal relationships, DCM has two levels of modeling: the first-level model estimates the causal relationships directly at the level of neural activities and the second-level model explicitly estimates how BOLD signals are generated from the modeled neural activities. Therefore, DCM is able to account for the heterogeneity of hemodynamic responses across regions (David et al., 2008). More specifically, in DCM, the effective connectivity parameters are estimated using the bilinear state equation as the following:

$$\dot{z} = \left( A + \sum_{j=1}^{M} u_j B^j \right) z + Cu \tag{1}$$

where $\dot{z}$ denotes the time derivative of neuronal activity which influenced by three factors: the A (intrinsic parameters) represents the intrinsic coupling among brain areas in the absence of external perturbations; $B^j$ (modulatory parameters) represents the change in connectivity induced by experimental context $u_j$ (e.g., experimental stimulation); $C$ (input parameters) embodies the perturbations of extrinsic inputs on neuronal activity ( Friston et al., 2003).

In the present study, we specified a full DCM with three regions (i.e., the contralateral thalamus, S1 and S2) for each session of each subject (Zeidman et al., 2019a). In a full DCM, all possible connectivity parameters were freely estimated, that is, there were bidirectional intrinsic connections between the thalamus and S1, between the thalamus and S2, and between S1 and S2, and all connections were allowed to be modulated by nociceptive and/or tactile stimuli. The external inputs (nociceptive and tactile stimuli) were exerted on the thalamus as a single combined input. After the full DCM model was estimated for each session of each subject, an average DCM was created for each subject by averaging the DCMs obtained from the two sessions using Bayesian averaging (Kasess et al., 2010).

### 2.6. Bayesian analyses at group level: parametric empirical Bayes and Bayesian model reduction

Parametric Empirical Bayes (PEB) and Bayesian Model Reduction ( Friston et al., 2015, 2016 ) were used to estimate the group-level effects. The PEB framework specifies a hierarchical statistical model of connectivity parameters:

$$y_i = \Gamma_i^{(1)}(\theta^{(1)}) + \epsilon_i^{(1)} \tag{2}$$

where $y_i$ is the observed fMRI data for subject $i$ which is generated by this subject's DCM function $\Gamma_i^{(1)}$, with parameters $\theta^{(1)}$ and observation noise $\epsilon_i^{(1)}$. The contribution of the PEB framework is that the DCM parameters $\theta^{(1)}$ are represented by a second-level model:

$$\theta^{(1)} = \Gamma^{(2)}(\theta^{(2)}) + \epsilon^{(2)} \tag{3}$$

$$\theta^{(2)} = \eta + \epsilon^{(3)} \tag{4}$$

where $\theta^{(2)}$ represents group-average connection strengths and $\epsilon^{(2)}$ represents between-subject variability. The second level parameters $\theta^{(2)}$ are further determined by priors, with mean $\eta$, and residuals $\epsilon^{(3)}$. Therefore, a PEB model was constructed for the group-level effects of all DCM parameters using the full posterior density over the parameters from each subject's DCM. In this way, PEB treats each parameter as a random effect which takes into account both the expected strength of each parameter and its associated uncertainty (i.e. posterior covariance). PEB is also computationally highly efficient and thus especially suitable in situations where there are many unknown parameters to estimate in a DCM. Indeed, if the conventional Bayesian model selection method (Stephan et al., 2009) were to be used to identify the best model with the highest exceedance probability from a pre-defined model space including all possible model structures as used in several previous DCM studies (Chung et al., 2014; Kalberlah et al., 2013; Khoshnejad et al., 2014; Liang et al., 2011), there would be at least 262,144 models to estimate and compare for each participant, which is computationally infeasible – there are nine intrinsic connections and four possible configurations of modulatory effects on each connection, that is, no modulatory effect, only modulated by nociceptive stimuli, only modulated by tactile stimuli, and modulated by both nociceptive and tactile stimuli ($n = 4^9$).

Once a group-level PEB model with a full connectivity configuration was obtained, a Bayesian model reduction (BMR) was used to prune away any insignificant connectivity parameters from the full connectivity model until the model evidence was not improved (see [Friston et al., 2016; Zeidman et al., 2019b] for details). In brief, this procedure compares the evidence for reduced models, iteratively discarding parameters that do not contribute to model evidence until the model evidence starts to decrease. Technically, this is known as a greedy search and allows thousands of models to be compared quickly and efficiently. In the present study, a connectivity parameter is considered as significant if its posterior probability $P > 0.95$. Paired t tests were also performed between nociceptive and tactile conditions to test whether nociceptive and tactile stimuli had significantly different modulatory effects on each of the connections within this 'thalamus-S1-S2' network.

### 2.7. Control analyses

To test the reliability of the results, we also performed three control analyses as follows. In Control Analysis 1, two separate input regressors (one for nociceptive stimuli and the other for tactile stimuli) were specified in each DCM, as opposed to a single input regressor combining nociceptive and tactile stimuli in the above main analysis. All other analysis procedure (i.e., DCM model estimation, PEB and BMR) were identical to

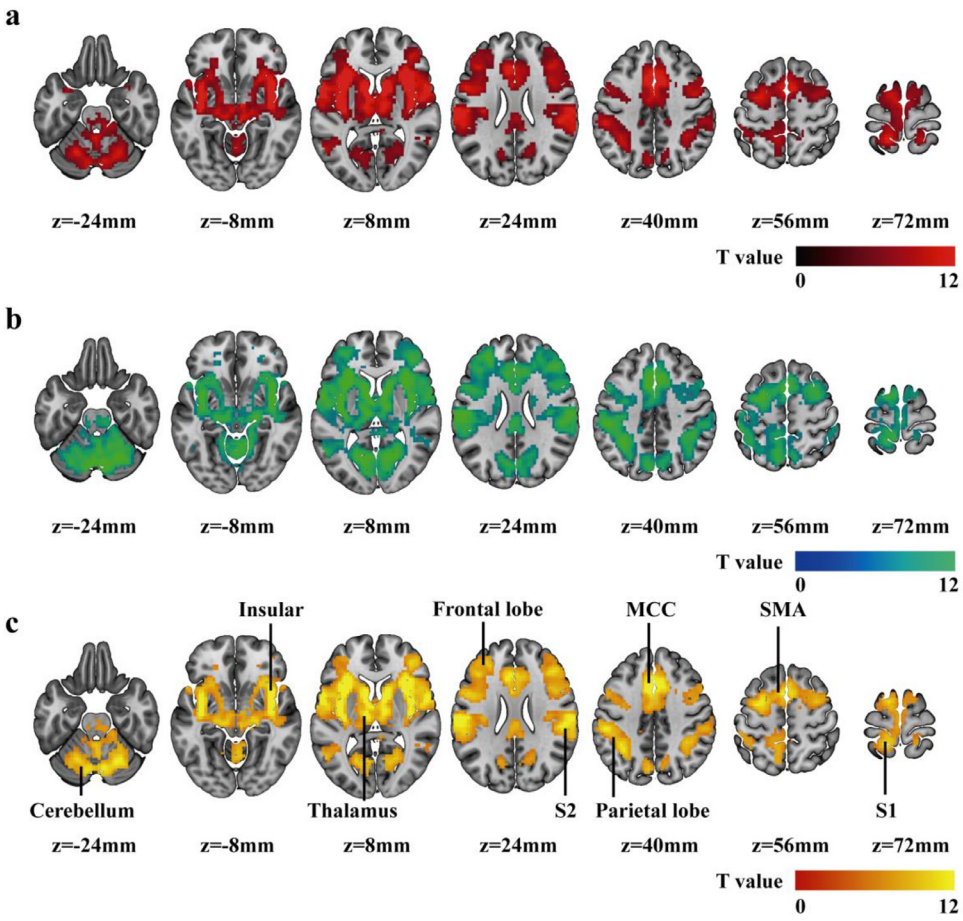


**Fig. 1.** Results of group-level general linear model analyses: the activation map of nociceptive stimuli (a), the activation map of tactile stimuli (b) and the co-activated map of nociceptive and tactile stimuli (c). These results were corrected by FWE at voxel level ($p<0.05$ corrected). S1, primary somatosensory cortex; S2, secondary somatosensory cortex; SMA, supplementary motor area; MCC, mid-cingulate cortex.

the main analysis. In Control Analysis 2, a more traditional hypothesis-driven, family-level BMS framework as implemented in (Zeidman et al., 2019b) was adopted, as opposed to the 'PEB + BMR' procedure performed in the main analysis. Using this family-level BMS framework, we tested each of the three questions of interest in the present study: (1) whether nociceptive or tactile stimuli are processed in a parallel or serial manner; (2) whether and how S1 activity modulates the thalamic activity; and (3) whether and how S2 activity modulates the thalamic activity. In Control Analysis 3, the stimulus intensity was also included in the DCM as an additional modulatory condition to test whether the modulatory effects of stimulus modality were dependent on stimulus intensity. The detailed methods for the three control analyses are provided in the Supplementary Methods.

## 3. Results

### 3.1. Behavioral data

For nociceptive stimuli, the group average of the physical intensities was 4.21 ± 0.99 J, and the group average of the perceived intensity (i.e., the subjective intensity ratings) was 4.16±2.03. For tactile stimuli, the group average of the physical intensities was 9.60±7.17 mA, and the group average of the perceived intensity was 4.35±1.73. The two-way repeated-measure ANOVA showed that there was a highly significant difference in subjective ratings between high- and low-level stimuli (main effect of 'intensity': $F = 296.54$, $P = 4.94 \times 10^{-44}$) but no significant difference between painful and tactile stimuli (main effect of 'modality': $F = 2.0$, $P = 0.15$) or significant interaction between the two factors ('modality × intensity': $F = 1.02$, $P = 0.31$).

### 3.2. General linear model analysis and ROI selection

Fig. 1 shows the brain areas activated by nociceptive stimuli (panel a), activated by tactile stimuli (panel b) and commonly activated by both stimuli (panel c). As shown in Fig. 1a&b, nociceptive and tactile stimuli activated very similar brain areas, in line with several previous studies (Liang et al., 2019; Mouraux et al., 2011; Su et al., 2019). Fig. 1c shows that the brain areas significantly responding to both nociceptive and tactile stimuli include the bilateral thalamus, S1, S2, insula, temporal superior lobe, inferior frontal lobe, supplementary motor area, mid-cingulate cortex, anterior cingulate cortex and cerebellum. The identified group-level peak voxels of the three ROIs (i.e., the thalamus, S1 and S2 contralateral to the stimulated side) were indicated in Figs. 2a (the white circles) and 2b (the red dots). The identified peak voxels of the three ROIs in each participant that were used in the subsequent individual-level DCM analyses are shown in Fig. 2b (the white dots). The mean BOLD time courses of each ROI and condition across the 57 participants are shown in Fig. 2c (red for nociceptive condition and blue for tactile condition).

### 3.3. DCM and Bayesian analyses

As shown in Fig. 3a, the intrinsic connections from the thalamus to S1, from the thalamus to S2 were significantly positive; the intrinsic connections from S1 to thalamus and from S1 to S2 were significantly negative. The intrinsic connections from S2 to thalamus and from S2 to S1 were not significant and the effect size was virtually zero (Fig. 3a). As shown in Fig. 3b, almost all modulatory parameters, except those on the feedback connection from S1 to thalamus, were significant. The posterior probability and posterior covariance for each estimated parameter

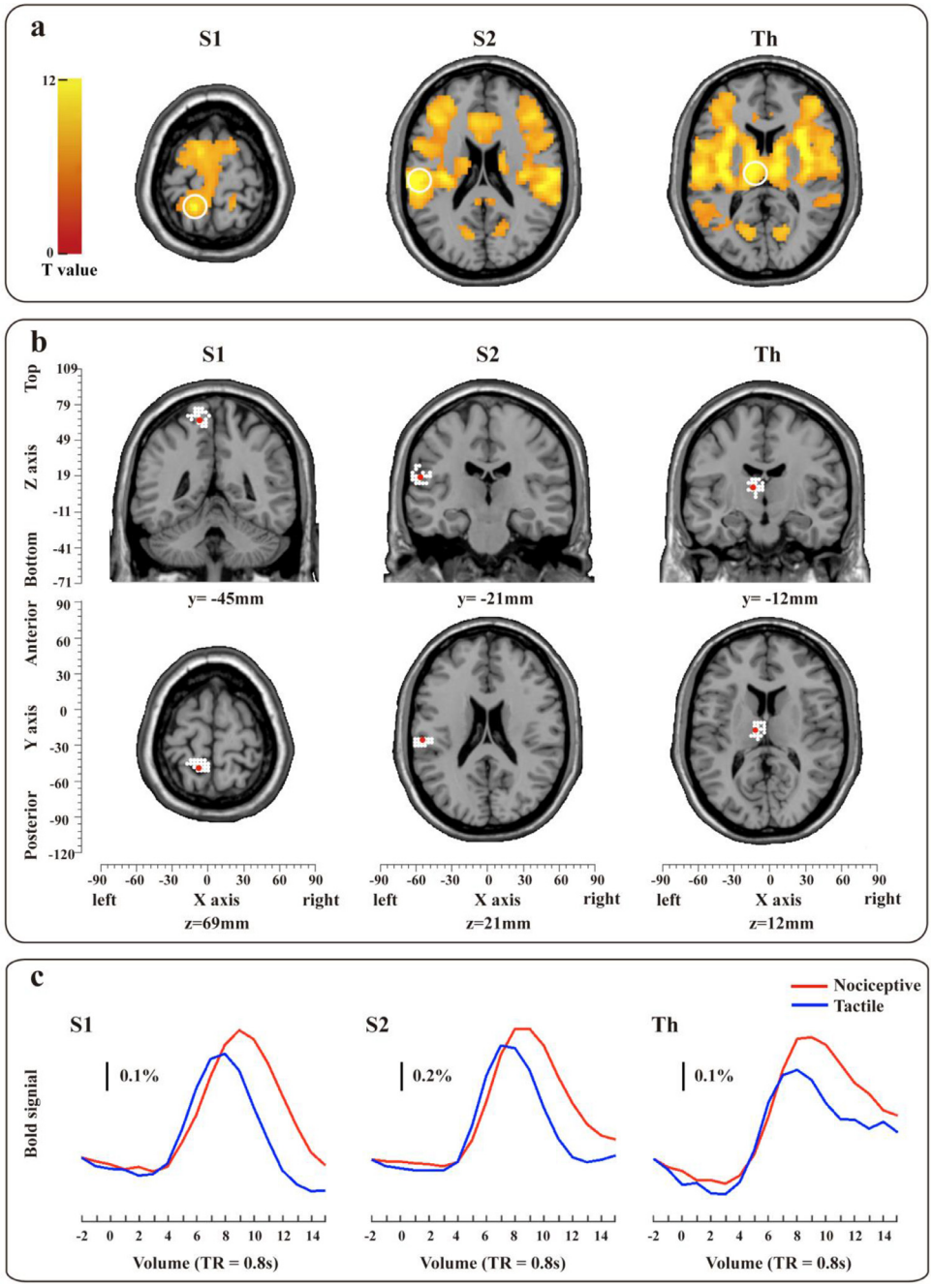


**Fig. 2.** Brain areas activated by nociceptive and tactile stimuli in the thalamus, S1 and S2 (contralateral to the stimulated side) for selecting the regions of interest (ROIs) at the group level (a) and at the individual level (b) and the corresponding mean BOLD time courses extracted from the three ROIs of the 57 subjects (c). The white circles in panel a and the red dots in panel b indicate the group-level peak voxels of the three ROIs, and the white dots in panel b indicate the peak voxels of the three ROIs in each individual participant. Lines in red and in blue in panel c correspond to the nociceptive and tactile conditions, respectively. The x-axis indicates peri-stimulus volumes sampled at TR=0.8 s. Th, thalamus; S1, primary somatosensory cortex; S2, secondary somatosensory cortex. (For interpretation of the references to color in this figure legend, the reader is referred to the web version of this article.)

are shown in Supplementary Table S1. The final model structure shown in Fig. 4 indicates that two feedforward connections from the thalamus to S1 and from thalamus to S2, bidirectional connections between S1 and S2, were modulated by both nociceptive and tactile stimuli, and all these modulatory effects are positive. Interestingly, the feedback connection from S2 to thalamus were negatively modulated by both nociceptive and tactile inputs and the effect sizes of the two modulatory parameters were similar with the modulatory effects on the corresponding feedforward connection (i.e., from the thalamus to S2), while the feedback connection from S1 to thalamus was not significantly modulated by any stimuli (Figs. 3&4). This result suggests that nociceptive and tactile stimuli had similar modulatory effects on the connections within this 'thalamus-S1-S2' network. Using the estimated individual DCMs, paired t tests further confirmed that there was no significant difference in the modulatory effects on any connection between nociceptive and tactile conditions ($P$>0.05, uncorrected) (the upper-right inset image of Fig. 4).

### 3.4. Control analyses

We observed similar results with the above main analysis in all control analyses. For Control Analysis 1, the results are shown in Supplemental Figs S1-S2. For Control Analysis 2, the results are shown in Supplemental Fig S5. For Control Analysis 3, the results are shown in Supplemental Figs S6-S7 and Supplemental Tables S3-S4.

## 4. Discussion

In the present study, we applied DCM in combination with PEB and BMR to fMRI data (TR = 0.8 s) to investigate the hierarchical organization for the processing of nociceptive and tactile information in the 'thalamus-S1-S2' network. Crucially, we modelled both feedforward and feedback pathways between the thalamus and S1/S2 in the DCM. There are three main findings: (1) our results support parallel ascending path-

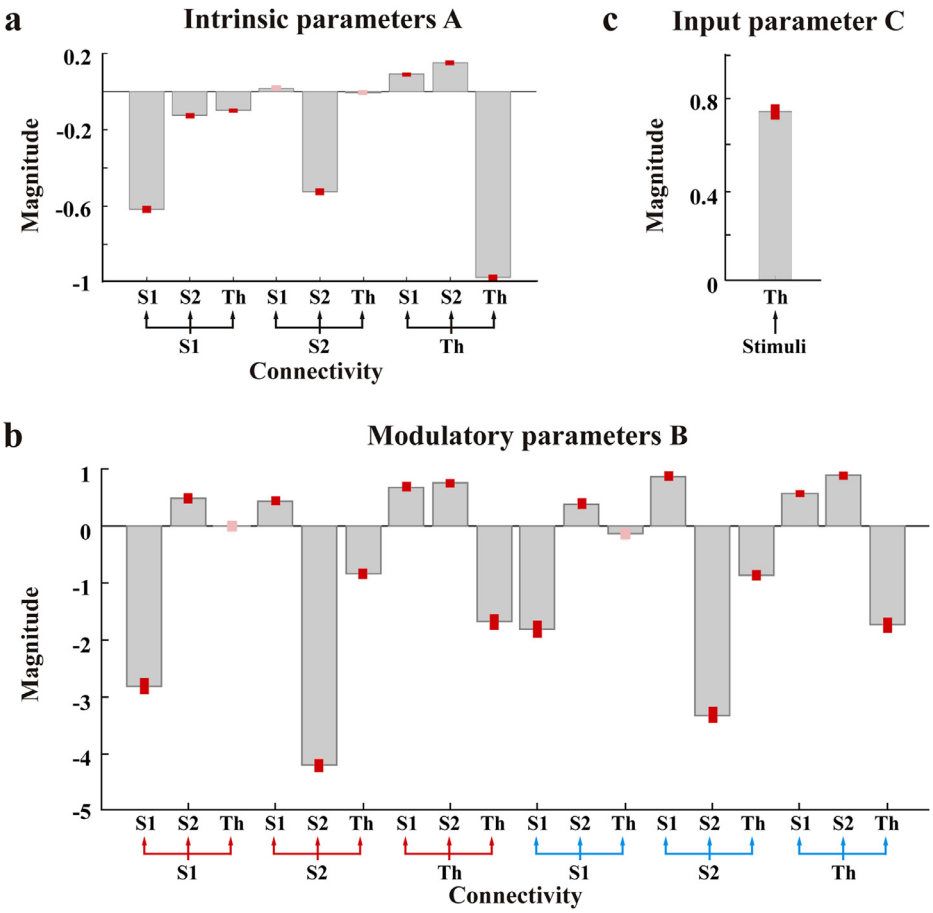


**Fig. 3.** The group mean estimated intrinsic parameters (a), modulatory parameters (b) and input parameter (c). Gray bars represent posterior means and pink bars (or red bars) represent 95% Bayesian confidence intervals. The red bars represents the parameters whose posterior probability >0.95. In the abscissa labeling of panel b, red represents nociceptive condition, and blue represents tactile condition. (For interpretation of the references to color in this figure legend, the reader is referred to the web version of this article.)

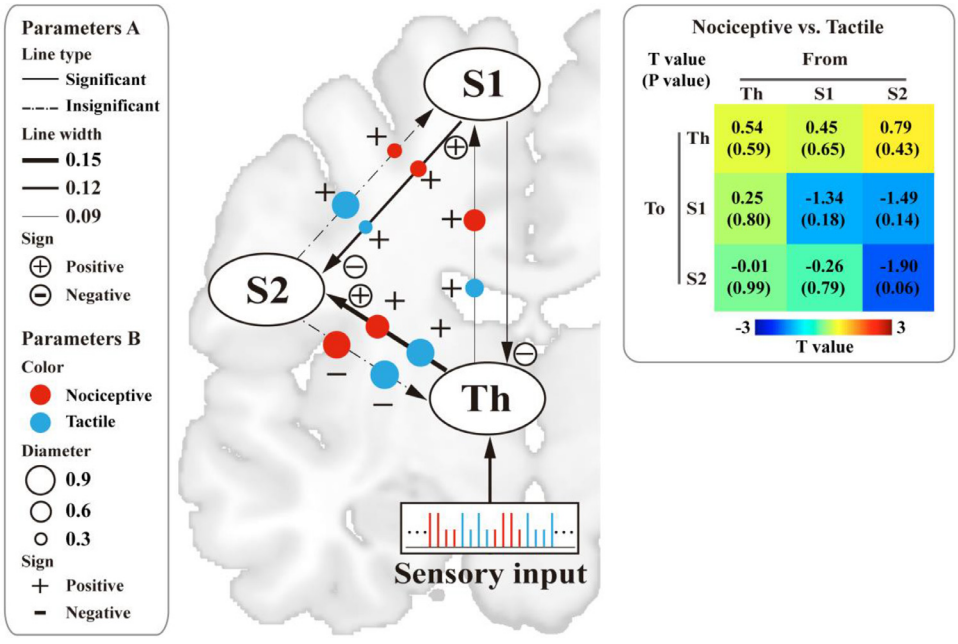


**Fig. 4.** Final model structure determined by PEB and BMR. Black lines with arrowhead represent the intrinsic connections in the 'thalamus-S1-S2' network and the thickness of the lines represent the magnitude of each connection (the solid lines represent significant intrinsic connections and the dotted lines represent insignificant intrinsic connections). Signs in circle beside the arrowhead indicate the sign of the intrinsic connection. Colored dots on black lines represent the modulatory parameters and the colors represent stimulus type (red represents nociceptive stimuli and blue represents tactile stimuli). The size of colored dots represents the magnitude of modulatory effects. Signs beside colored dots indicate the sign of modulation effects. The upper-right inset image shows the results (T and P values) of comparisons of the modulatory parameters (i.e., parameters B) between nociceptive and tactile conditions obtained from paired t tests. The 'thalamus-S1-S2' network is shown as a matrix and each entry corresponds to a connectivity; for example, the entry of the third row and the first column corresponds to the connectivity from thalamus to S2. The color of each entry indicates the T value which is also shown inside each entry, along with the corresponding P value (uncorrected). Th, thalamus; S1, primary somatosensory cortex; S2, secondary somatosensory cortex. (For interpretation of the references to color in this figure legend, the reader is referred to the web version of this article.)

ways from the thalamus to both S1 and S2 for nociceptive as well as tactile information transmission; (2) the corticothalamic feedback within this 'thalamus-S1-S2' network is reflected by a negative intrinsic connectivity from S1 to thalamus without modulation by external stimuli and a negative modulatory effect on the connectivity from S2 to thalamus by both nociceptive and tactile stimuli; and (3) the hierarchy of the information flow within the 'thalamus-S1-S2' somatosensory network are similar for nociceptive and tactile processing.

### *4.1. Parallel ascending pathways for nociceptive and tactile inputs in the 'thalamus-S1-S2' network*

In the present study, the observations of significant intrinsic connectivity from the thalamus to both S1 and S2 and, importantly, the corresponding modulatory effects of nociceptive and tactile inputs suggest that the nociceptive and tactile information are processed in parallel in S1 and S2 with a bifurcated input from the thalamus (Fig. 4). Moreover, both the estimated intrinsic and modulatory parameters of these two feedforward pathways were positive, which suggests that thalamic activity had an excitatory effect on S1 and S2 and this effect was further enhanced during nociceptive and tactile stimulation. This finding is consistent with the results of several previous studies suggesting parallel processing for nociceptive (Chung et al., 2014; Liang et al., 2011) and/or tactile information (Liang et al., 2011). In fact, evidence of direct anatomical connections from the thalamus to both S1 and S2 has long been established. For example, early animal studies have reported that several thalamic nuclei such as the ventroposterior lateral (VPL) nucleus and the ventroposterior inferior (VPI) nucleus project not only to S1 but also to S2 in rhesus monkeys (Burton and Jones, 1976) and macaques (Friedman and Murray, 1986). A more recent study reported that the thalamic projections to S2 were even denser (30%) compared with those to S1 (<5%) using anterograde transneuronal transit of herpes simplex virus in monkeys (Dum et al., 2009). All these evidence indicate that one of the major inputs to S2 is directly from the thalamus.

Given the established anatomical basis for parallel transmission from the thalamus to S1 and S2, the functional evidence so far, despite only a few, mostly support parallel processing of nociceptive information in S1 and S2. These evidence are mainly from MEG studies showing similar response onset times in S1 and S2 after nociceptive stimulation (Kanda et al., 2000; Ploner et al., 1999, 2009) and a fMRI-DCM study showing parallel modulation of nociceptive stimuli on the pathways from the thalamus to both S1 and S2 (Liang et al., 2011). As there are several intrinsic limitations of MEG technique such as (1) insensitivity to deep sources, (2) over-simplified head model and infinite number of solutions during source reconstruction, and (3) possible differences in conduction velocity of the thalamocortical pathways to S1 and S2 and/or in neuronal response time between S1 and S2 ( Trappenberg, 2002), fMRI-DCM may be preferred in making inferences about the hierarchy of information transmission. Consistent with our previous study (Liang et al., 2011), the results of the present study provide a stronger evidence showing again a parallel modulation of nociceptive stimuli on the two thalamocortical pathways using a much higher resolution (0.8 s vs. 3 s), a larger sample size (57 subjects vs. 14 subjects) and when the feedback pathways were also included in the DCM. It should be noted that one previous DCM study reported contradicting results showing that the 'serial' models with only the extrinsic input to S1 (rather than the 'parallel' models with extrinsic inputs to both S1 and S2) had the highest exceedance probability (Khoshnejad et al., 2014). However, unlike the laser stimuli used in the present study that selectively activate nociceptors (i.e., A$\delta$ fibers), their noxious stimuli were high-intensity electrical pulses which activate not only nociceptive (i.e., A$\delta$ fibers) but tactile (i.e., A$\beta$ fibers) receptors. Therefore, their results might have been confounded by concurrent nociceptive and tactile processing and, more importantly, their interaction that has been shown to be highly complicated in nature (Apkarian et al., 1994; Mancini et al., 2015). Furthermore, in this previous study, the 'serial vs. parallel' hypotheses were tested by exerting the extrinsic inputs directly to S1 and S2 without including the thalamus (Khoshnejad et al., 2014). Missing this key region (i.e., the thalamus) in their DCM might also explain the discrepancy between the results of this previous study and our present study.

In contrast with the previous evidence mostly supporting parallel processing for nociceptive information, previous evidence about the hierarchy of tactile processing are much more inconsistent. Evidence supporting the 'serial' hypothesis for tactile processing mainly consists of three types of studies. First, a reduction of responses in S2 was observed after the ablation of S1 in higher primates, suggesting that the responses in S2 is dependent on the responses in S1 (Pons et al., 1992). Second, the responses in S2 appeared later than those in S1 by intracranial recording or source reconstruction of MEG data in human, suggesting a temporal precedence of information processing in S1 over S2 (Hari et al., 1993; Inui et al., 2004; Mima et al., 1998; Ploner et al., 2009; Schnitzler et al., 1999). Third, models depicting a serial processing of tactile information showed highest probability compared to models depicting a parallel processing by DCM analysis of human fMRI data (Kalberlah et al., 2013; Khoshnejad et al., 2014). However, all these lines of evidence are not unequivocal. As pointed before (Liang et al., 2011), the dependence of responses in S2 on responses in S1 does not exclude the parallel processing of tactile information in both S1 and S2 because such dependence can be achieved via the additional connectivity between S1 and S2. Indeed, our present and previous studies (Liang et al., 2011) showed a significant intrinsic connectivity from S1 to S2 and a significant modulatory effect on this connectivity during tactile processing. Furthermore, as mentioned above, temporal precedence of neural responses in S1 over S2 does not necessarily imply serial processing from S1 to S2 because it can be confounded by many other factors such as conduction velocities and/or oversimplified assumptions during source reconstruction (Trappenberg, 2002). In addition, missing the key region, the thalamus, in the DCMs also made them unable to test directly the ascending pathways from the thalamus to S1 and S2 in these previous studies (Kalberlah et al., 2013; Khoshnejad et al., 2014). Evidence supporting 'parallel' hypothesis for tactile processing also exist. In addition to two other DCM studies reporting similar results (Chung et al., 2014; Liang et al., 2011) with our present study, there are also other types of evidence showing (1) that responses in S2 were not completely abolished after the ablation of S1 (Pons et al., 1992) or even largely unaffected by the inactivation of S1 by cooling in higher primates (Zhang et al., 1996); (2) patients with lesions of the parietal cortex encompassing S1 had largely unaffected perception of somatosensory qualities like vibration (Knecht et al., 1996); and (3) the earliest responses in S2 peaked at 20–30 ms after the onset of tactile stimuli, which was compatible with the peak latency of responses in S1 (Karhu and Tesche, 1999). Taken all these findings and our present finding together, it suggests a parallel processing for tactile information in the 'thalamus-S1-S2' network.

It is worth noting that the observation that S2 receives direct inputs from the thalamus for nociceptive and tactile processing does not mean that the nociceptive/tactile processing in S1 and S2 are independent. In fact, previous studies have reported the information transmission between S1 and S2 (Hu et al., 2012; Gao et al., 2015), which is in line with the observed intrinsic and modulatory connectivities between S1 and S2 in the present study. Our results further showed that the significantly negative intrinsic connectivity from S1 to S2 and the insignificant intrinsic connectivity from S2 to S1 were positively modulated by both nociceptive and tactile stimuli with much larger amplitudes (i.e., the positive modulatory effects were much larger than the amplitudes of these two intrinsic connectivity) (see Supplementary Table S1). Therefore, it appears that the activities in S1 and S2 had an excitatory effect on each other during nociceptive and tactile stimulation. These observations highlight that nociceptive/tactile information is also transmitted from the S1 to S2 in addition to the direct transmission from the thalamus to S2. Another possible explanation of the contradicting results about 'serial vs. parallel' hypotheses is that the hierarchy of the so-

matosensory processing might change over time (Klingner et al., 2015, 2016) which cannot be verified using the current methodology adopted in the present study.

### 4.2. Distinct feedback regulations of S1 and S2 on the thalamus during somatosensory processing

Compared with the previous studies, one of the strengths of the present study is that the descending pathways from the S1 and S2 to the thalamus were also taken into account in the constructed DCMs, enabling the investigation of possible corticothalamic feedback regulations within this 'thalamus-S1-S2' network. Indeed, the existence of corticothalamic pathways have been reported in abundant anatomical studies in animals showing that both S1 and S2 send fibers to various thalamic nuclei especially the posterior nuclei of the thalamus (Auer, 1956; Chmielowska et al., 1989; Jones and Powell, 1968, 1970; Liao et al., 2010; Niimi et al., 1963; Nothias et al., 1988; Rinvik, 1968a, b; Spreafico et al., 1987; Stratford, 1954; Veinante et al., 2000). Anatomical evidence showed that corticothalamic projections are ~10 times more numerous than thalamocortical projections (Liu et al., 1995). For example, using strychnine neuronography, Stratford and colleagues demonstrated corticothalamic connections originated from the S1 and S2 in the cat – S1 projects to the nucleus VPLc, while S2 projects to the caudal extension of nucleus ventralis posteromedialis (Stratford, 1954). Such finding was also extended to the monkeys showing that the corticothalamic fibers project from S1 and S2 in an organized manner to the ventroposterior nucleus (Jones and Powell, 1970). Given these anatomical evidence of the descending pathways, many animal studies have also tried to address their functions during somatosensory processing (Fanselow et al., 2001; Mo and Sherman, 2019; Monconduit et al., 2006; Temereanca and Simons, 2004; Wang et al., 2007). However, all these studies mainly focused on the regulatory effects of S1, but not S2, on thalamic activities, and reported both excitatory and inhibitory effects during noxious or tactile processing. For example, one study examined the effect of enhancement of corticothalamic activity in S1 on the whisker-evoked responses in topographically aligned thalamic barreloid neurons in rodents and found that S1 could selectively regulate thalamic spatial response tuning by engaging topographically specific excitatory and inhibitory mechanisms in the thalamus (Temereanca and Simons, 2004). Furthermore, applying microinjections within S1 for pharmacological manipulation of corticofugal modulation, Monconduit et al. reported that Glutamatergic activation of corticofugal output enhanced noxious-evoked responses and affected in a biphasic way tactile-evoked responses of VPLc, while $GABA_A$-mediated depression of corticofugal output concomitantly depressed noxious-evoked and enhanced innocuous-evoked responses of VPL neurons (Monconduit et al., 2006). However, these functional studies using animals are generally very challenging because (1) the results obtained from anesthetized animals may not reflect the functions in natural state since sensory responses of corticothalamic neurons can be significantly inhibited during anesthesia (Alitto and Usrey, 2015; Briggs and Usrey, 2011) and (2) the complex nature of the specific spatial locations and temporal structure of the feedback signals also aggravates the difficulty of studying feedback regulations (Briggs and Usrey, 2009; Granseth et al., 2002; Li et al., 2003).

In the present study, we addressed this question by examining the intrinsic connections from S1 and S2 to the thalamus and the corresponding modulatory effects of external stimuli on these connections based on DCM of human fMRI data. Our results clearly revealed the existence of the corticothalamic regulation from both S1 and S2 but the regulatory effects originated from S1 and S2 are distinct – there was a significantly negative intrinsic connectivity from S1 to the thalamus and this connection was not significantly modulated by somatosensory inputs, while the intrinsic connectivity from S2 to the thalamus was not significant but there was a strong, negative modulatory effects of the external inputs on this connection (Fig. 4). Interestingly, a recent electrophysiological study in monkeys reported a very similar result regarding the bidirectional connections between the thalamus and S1 – using simultaneous recording of neurons sharing the same cutaneous receptive field in VPL and S1 while monkeys judged the presence or absence of tactile stimuli, Campo et al. found that, compared with the period of stimulus absence, the feedforward (i.e., VPL-S1) information increased as a function of stimulus amplitude but the feedback (i.e., S1-VPL) information was unchanged during the presence of stimuli (Tauste Campo et al., 2019). These findings indicate that both S1 and S2 exert inhibitory effects on the neural activity of the thalamus, but the inhibitory effects of S1 on the thalamus is more constant and not dependent on the occurrence of external stimuli whereas the inhibitory effects of S2 on the thalamus only appear during external stimulation. It has been shown that neurons in the cortical layer VI send feedback projections to the thalamus via monosynaptic and disynaptic projections. More specifically, the monosynaptic excitatory effect is achieved through glutamatergic synapses, whereas disynaptic pathway drives GABAergic neurons of the thalamic reticular nucleus which, in turn, provide inhibitory input onto the relay neurons of the thalamus (Murray Sherman and Guillery, 2001). Our observation of the distinct feedback regulations from S1 and S2 to the thalamus further suggests that the inhibitory corticothalamic feedback regulation is mainly originated from S1 in baseline state but S2, as a higher level somatosensory area, provides additional inhibition to the thalamic activity once a somatosensory input is received to help recover resting potential of thalamic cells to control the firing mode of thalamic relay cells (Sherman, 2016). It should be noted that the current spatial and temporal resolution of the human fMRI data can only provide information about the corticothalamic feedback regulations on a macro-scale level but unable to characterize in detail on a micro-scale level the complex spatial pattern or temporal dynamics of feedback modulations from somatosensory cortices to thalamus.

It is also worth noting that, compared with the feedforward and feedback connections, the self-connections of the three regions had much larger amplitudes for both the intrinsic and modulatory parameters (Fig. 3b, Supplementary Table S1). Biologically, the self-connection of a given region can be interpreted as controlling the excitatory-inhibitory balance of its own activity, mediated by the interaction of pyramidal cells and inhibitory interneurons (Bastos et al., 2012; Zeidman et al., 2019a). According to Eq. (3) in (Zeidman et al., 2019a), a self-connection is always inhibitory – a positive self-connection indicates an enhanced inhibition and a negative self-connection indicates a reduced inhibition. Therefore, the self-connection of a region affects its responsiveness to the inputs from other regions or to the external stimuli – the more positive a self-connection, the less responsive the given region to other inputs; conversely, the more negative a self-connection, the more responsive the given region to other inputs (Zeidman et al., 2019a). In our results, all intrinsic self-connections were significantly negative and were further negatively modulated by nociceptive and tactile stimuli (Fig. 3b, Supplementary Table S1), suggesting that these regions were disinhibited and became more responsive to the inputs from other regions of the network during nociceptive and tactile stimulation.

### 4.3. Similar processing hierarchy of nociceptive and tactile information flow within the 'thalamus-S1-S2' network

Our results suggest that the network hierarchy of both the ascending and descending pathways within the 'thalamus-S1-S2' system were very similar during nociceptive and tactile information processing (Fig. 4). The observation of no significant difference in the magnitudes of modulatory effects on any connectivity between the two conditions (the upper-right inset image of Fig. 4) also supports that they may share a similar network organization. These findings are consistent with our previous study (Liang et al., 2011) which also suggested similar hierarchy (i.e., parallel ascending pathways) during nociceptive and tactile processing. Note that, compared with our previous study, the methodology adopted in the present study is quite different in some technical aspects: much higher temporal resolution, the inclusion of corticotha-

lamic descending pathways, and the use of PEB and BMR rather than Bayesian model selection during the DCM analysis. The fact that we still observed similar results despite these methodological differences indicates the robustness of this finding.

### 4.4. Limitations

There are several limitations in the present study. First, the evidence obtained from fMRI-DCM is not definitive for solving the problem of information flow among different brain regions due to the fact that it measures hemodynamic responses rather than neural activity directly. However, DCM combined with fMRI is one of the most feasible techniques to study the network organization in a living human brain to date considering that (1) direct electrophysiological recordings in a normal human brain is very difficult in practice, (2) anatomical connections do not necessarily correspond to the true signal transmission pathways in a certain functional state (e.g., pain state), and (3) fMRI-DCM adopts a two-level modeling to infer the effective connectivity on neural level – a connectivity model constructed and estimated on neuronal level and a hemodynamic response model for transforming neural activity to BOLD responses. With the development of ultrahigh-field MRI techniques, fMRI data acquired using layer-specific imaging with 7-T MRI may be used to confirm the current results in future studies. Second, although the thalamocortical projections to S1 and S2 involve multiple lateral and central thalamic nuclei (Friedman and Murray, 1986; Jones, 1998; Krubitzer and Kaas, 1992), the limited spatial resolution of fMRI did not allow us to accurately localize the most relevant nucleus, VPL, in the thalamocortical transmission of somatosensory information. Third, although certain measures have been taken into account for HRF variability (e.g., the temporal derivatives of the hemodynamic responses for each type of stimuli were included in GLM; and the hemodynamic response is modeled by a nonlinear input–state–output model with hyperparameters modeling how the regional cerebral blood flow changes with neuronal activity in DCM), the confounding effect related to the peripheral conduction velocity cannot be completely removed in the present study. Fourth, due to the high computational load of the DCM estimation, we only included the most relevant brain regions (i.e., thalamus, S1 and S2) in our DCM. However, other regions such as insula, cingulate cortex, several areas in the frontal and parietal lobes, and cerebellum are also involved in the somatosensory processing (Hu et al., 2012; Zhang et al., 2016; Tracey and Mantyh, 2007; Del Vecchio et al., 2019). Missing these regions in the DCM might have influenced the estimation of the effective connectivity within the 'thalamus-S1-S2' network. Fifth, although the results of the Control Analysis 3 did not show clear evidence for a significant effect of stimulus intensity on the connectivity of the 'thalamus-S1-S2' network, it should be noted that the statistical power of this control analysis was much lower than the main analysis (because the number of trials in each condition was only half of those in the main analysis), and thus we cannot rule out the possibility that the current statistical power was not sufficient to reveal a significant effect of stimulus intensity.

## Conclusions

Our findings obtained from dynamic causal modeling of fMRI data suggest that nociceptive and tactile information processing may share similar hierarchical organization within the 'thalamus-S1-S2' network: Nociceptive and tactile processing are likely to adopt a parallel hierarchy along the ascending thalamocortical pathways from the thalamus to both S1 and S2; however, the corticothalamic feedback regulations from the S1 and S2 to the thalamus are likely to be distinct – S1 generally exerts inhibitory corticothalamic feedback regulation independent of external stimulation whereas S2 provides additional inhibition to the thalamic activity during external stimulation. These findings provide important insights on how nociceptive and tactile information is hierarchically processed within the somatosensory system in the human brain.

## Credit author statement

**Yingchao Song:** Conceptualization, Methodology, Formal analysis, Investigation, Writing - original draft, Visualization. **Qian Su:** Data curation, Investigation. **Qingqing Yang:** Methodology, Investigation. **Rui Zhao:** Investigation. **Guotao Yin:** Investigation; Visualization. **Wen Qin:** Data curation, Investigation, Funding acquisition. Gian Domenico **Iannetti:** Writing-Review and Editing. **Chunshui Yu:** Supervision, Funding acquisition. **Meng Liang:** Conceptualization, Data curation, Funding acquisition, Methodology, Investigation, Project administration, Supervision, Writing-Review and Editing.

## Data and code availability statement

Most of the analyses in this study were performed using SPM12 interface. Other scripts we used have been uploaded as Supplementary Materials.

## Ethics statement

All participants provided written informed consent prior to the experiment, and the experimental procedures were approved by the Medical Research Ethics Committee of Tianjin Medical University General Hospital.

## Declaration of Competing Interest

The authors declare no competing financial interests.

## Acknowledgments

This work was supported by National Key Research and Development Program of China (2018YFC1314300 to CSY); National Natural Science Foundation of China (81971694 and 81571659 to ML, 82030053 to CSY, 81971599 and 81771818 to WQ); Natural Science Foundation of Tianjin City (19JCYBJC25100 to WQ); Tianjin Key Technology Research and Development Program (17ZXMFSY00090 to CSY).

## Supplementary materials

Supplementary material associated with this article can be found, in the online version, at doi:10.1016/j.neuroimage.2021.117957.

## References

Alitto, H.J., Usrey, W.M., 2015. Dissecting the dynamics of corticothalamic feedback. Neuron 86 (3), 605–607. doi:10.1016/j.neuron.2015.04.016.

Allison, T., McCarthy, G., Luby, M., Puce, A., Spencer, D.D., 1996. Localization of functional regions of human mesial cortex by somatosensory evoked potential recording and by cortical stimulation. Electroencephalogr Clin Neurophysiol. 100 (2), 126–140. doi:10.1016/0013-4694(95)00226-x.

Allison, T., McCarthy, G., Wood, C.C., Darcey, T.M., Spencer, D.D., Williamson, P.D., 1989a. Human cortical potentials evoked by stimulation of the median nerve. I. Cytoarchitectonic areas generating short-latency activity. J. Neurophysiol. 62 (3), 694–710. doi:10.1152/jn.1989.62.3.694.

Allison, T., McCarthy, G., Wood, C.C., Williamson, P.D., Spencer, D.D., 1989b. Human cortical potentials evoked by stimulation of the median nerve. II. Cytoarchitectonic areas generating long-latency activity. J. Neurophysiol. 62 (3), 711–722. doi:10.1152/jn.1989.62.3.711.

Apkarian, A.V., Stea, R.A., Bolanowski, S.J., 1994. Heat-induced pain diminishes vibrotactile perception: a touch gate. Somatosens. Mot. Res. 11 (3), 259–267. doi:10.3109/08990229409051393.

Auer, J., 1956. Terminal degeneration in the diencephalon after ablation of frontal cortex in the cat. J. Anat. 90 (1), 30–41.

Bastos, A.M., Usrey, W.M., Adams, R.A., Mangun, G.R., Fries, P., Friston, K.J., 2012. Canonical microcircuits for predictive coding. Neuron 76 (4), 695–711. doi:10.1016/j.neuron.2012.10.038.

Beauchamp, M.S., Laconte, S., Yasar, N., 2009. Distributed representation of single touches in somatosensory and visual cortex. Hum. Brain Mapp. 30 (10), 3163–3171. doi:10.1002/hbm.20735.

Briggs, F., Usrey, W.M., 2009. Parallel processing in the corticogeniculate pathway of the macaque monkey. Neuron 62 (1), 135–146. doi:10.1016/j.neuron.2009.02.024.

Briggs, F., Usrey, W.M., 2011. Corticogeniculate feedback and visual processing in the primate. J. Physiol. 589 (Pt 1), 33–40. doi:10.1113/jphysiol.2010.193599.
Burton, H., Carlson, M., 1986. Second somatic sensory cortical area (SII) in a prosimian primate, Galago crassicaudatus. J. Comp. Neurol. 247 (2), 200–220. doi:10.1002/cne.902470206.
Burton, H., Jones, E.G., 1976. The posterior thalamic region and its cortical projection in New World and Old World monkeys. J. Comp. Neurol. 168 (2), 249–301. doi:10.1002/cne.901680204.
Button, K.S., Ioannidis, J.P., Mokrysz, C., Nosek, B.A., Flint, J., Robinson, E.S., Munafo, M.R., 2013. Power failure: why small sample size undermines the reliability of neuroscience. Nat. Rev. Neurosci. 14 (5), 365–376. doi:10.1038/nrn3475.
Chmielowska, J., Carvell, G.E., Simons, D.J., 1989. Spatial organization of thalamocortical and corticothalamic projection systems in the rat SmI barrel cortex. J. Comp. Neurol. 285 (3), 325–338. doi:10.1002/cne.902850304.
Chung, Y.G., Han, S.W., Kim, H.S., Chung, S.C., Park, J.Y., Wallraven, C., Kim, S.P., 2014. Intra- and inter-hemispheric effective connectivity in the human somatosensory cortex during pressure stimulation. BMC Neurosci. 15, 43. doi:10.1186/1471-2202-15-43.
Cruccu, G., Pennisi, E., Truini, A., Iannetti, G.D., Romaniello, A., Le Pera, D., Valeriani, M., 2003. Unmyelinated trigeminal pathways as assessed by laser stimuli in humans. Brain 126 (Pt 10), 2246–2256. doi:10.1093/brain/awg227.
David, O., Guillemain, I., Saillet, S., Reyt, S., Deransart, C., Segebarth, C., Depaulis, A., 2008. Identifying neural drivers with functional MRI: an electrophysiological validation. PLoS Biol. 6 (12), 2683–2697. doi:10.1371/journal.pbio.0060315.
Del Vecchio, M., Caruana, F., Sartori, I., Pelliccia, V., Lo Russo, G., Rizzolatti, G., Avanzini, P., 2019. Ipsilateral somatosensory responses in humans: the tonic activity of SII and posterior insular cortex. Brain Struct. Funct, 224 (1), 9–18. doi:10.1007/s00429-018-1754-6.
Dum, R.P., Levinthal, D.J., Strick, P.L., 2009. The spinothalamic system targets motor and sensory areas in the cerebral cortex of monkeys. J. Neurosci. 29 (45), 14223–14235. doi:10.1523/JNEUROSCI.3398-09.2009.
Fanselow, E.E., Sameshima, K., Baccala, L.A., Nicolelis, M.A., 2001. Thalamic bursting in rats during different awake behavioral states. Proc. Natl. Acad. Sci. U. S. A. 98 (26), 15330–15335. doi:10.1073/pnas.261273898.
Forss, N., Jousmaki, V., 1998. Sensorimotor integration in human primary and secondary somatosensory cortices. Brain Res. 781 (1–2), 259–267. doi:10.1016/s0006-8993(97)01240-7.
Friedman, D.P., Jones, E.G., Burton, H., 1980. Representation pattern in the second somatic sensory area of the monkey cerebral cortex. J. Comp. Neurol. 192 (1), 21–41. doi:10.1002/cne.901920103.
Friedman, D.P., Murray, E.A., 1986. Thalamic connectivity of the second somatosensory area and neighboring somatosensory fields of the lateral sulcus of the macaque. J. Comp. Neurol. 252 (3), 348–373. doi:10.1002/cne.902520305.
Friston, K., Zeidman, P., Litvak, V., 2015. Empirical Bayes for DCM: a Group Inversion Scheme. Front. Syst. Neurosci. 9, 164. doi:10.3389/fnsys.2015.00164.
Friston, K.J., Harrison, L., Penny, W., 2003. Dynamic causal modelling. Neuroimage 19 (4), 1273–1302. doi:10.1016/s1053-8119(03)00202-7, S1053811903002027 [pii].
Friston, K.J., Litvak, V., Oswal, A., Razi, A., Stephan, K.E., van Wijk, B.C.M., Zeidman, P., 2016. Bayesian model reduction and empirical Bayes for group (DCM) studies. Neuroimage 128, 413–431. doi:10.1016/j.neuroimage.2015.11.015.
Gao, L., Sommerlade, L., Coffman, B., Zhang, T., Stephen, J.M., Li, D., Schelter, B., 2015. Granger causal time-dependent source connectivity in the somatosensory network. Sci. Rep. 5, 10399. doi:10.1038/srep10399.
Garraghty, P.E., Florence, S.L., Tenhula, W.N., Kaas, J.H., 1991. Parallel thalamic activation of the first and second somatosensory areas in prosimian primates and tree shrews. J. Comp. Neurol. 311 (2), 289–299. doi:10.1002/cne.903110209.
Gingold, S.I., Greenspan, J.D., Apkarian, A.V., 1991. Anatomic evidence of nociceptive inputs to primary somatosensory cortex: relationship between spinothalamic terminals and thalamocortical cells in squirrel monkeys. J. Comp. Neurol. 308 (3), 467–490. doi:10.1002/cne.903080312.
Goebel, R., Roebroeck, A., Kim, D.S., Formisano, E., 2003. Investigating directed cortical interactions in time-resolved fMRI data using vector autoregressive modeling and Granger causality mapping. Magn. Reson. Imaging 21 (10), 1251–1261. doi:10.1016/j.mri.2003.08.026.
Granseth, B., Ahlstrand, E., Lindstrom, S., 2002. Paired pulse facilitation of corticogeniculate EPSCs in the dorsal lateral geniculate nucleus of the rat investigated in vitro. J. Physiol. 544 (2), 477–486. doi:10.1113/jphysiol.2002.024703.
Guillery, R.W., 1967. Patterns of fiber degeneration in the dorsal lateral geniculate nucleus of the cat following lesions in the visual cortex. J. Comp. Neurol. 130 (3), 197–221. doi:10.1002/cne.901300303.
Hari, R., Karhu, J., Hamalainen, M., Knuutila, J., Salonen, O., Sams, M., Vilkman, V., 1993. Functional organization of the human first and second somatosensory cortices: a neuromagnetic study. Eur. J. Neurosci. 5 (6), 724–734. doi:10.1111/j.1460-9568.1993.tb00536.x.
Hu, L., Iannetti, G.D., 2016. Painful Issues in Pain Prediction. Trends Neurosci. 39 (4), 212–220. doi:10.1016/j.tins.2016.01.004.
Hu, L., Zhang, Z.G., Hu, Y, 2012. A time-varying source connectivity approach to reveal human somatosensory information processing. Neuroimage 62 (1), 217–228. doi:10.1016/j.neuroimage.2012.03.094.
Iannetti, G.D., Truini, A., Romaniello, A., Galeotti, F., Rizzo, C., Manfredi, M., Cruccu, G., 2003. Evidence of a specific spinal pathway for the sense of warmth in humans. J. Neurophysiol. 89 (1), 562–570. doi:10.1152/jn.00393.2002.
Inui, K., Wang, X., Tamura, Y., Kaneoke, Y., Kakigi, R., 2004. Serial processing in the human somatosensory system. Cereb. Cortex 14 (8), 851–857. doi:10.1093/cercor/bhh043.
Iwamura, Y., 1998. Hierarchical somatosensory processing. Curr. Opin. Neurobiol. 8 (4), 522–528. doi:10.1016/s0959-4388(98)80041-x.
Jones, E.G., 1998. Viewpoint: the core and matrix of thalamic organization. Neuroscience 85 (2), 331–345. doi:10.1016/s0306-4522(97)00581-2.
Jones, E.G., Powell, T.P., 1968. The projection of the somatic sensory cortex upon the thalamus in te cat. Brain Res. 10 (3), 369–391. doi:10.1016/0006-8993(68)90206-0.
Jones, E.G., Powell, T.P., 1970. Connexions of the somatic sensory cortex of the rhesus monkey. 3. Thalamic connexions. Brain 93 (1), 37–56. doi:10.1093/brain/93.1.37.
Kalberlah, C., Villringer, A., Pleger, B., 2013. Dynamic causal modeling suggests serial processing of tactile vibratory stimuli in the human somatosensory cortex–an fMRI study. Neuroimage 74, 164–171. doi:10.1016/j.neuroimage.2013.02.018.
Kanda, M., Nagamine, T., Ikeda, A., Ohara, S., Kunieda, T., Fujiwara, N., . . . Shibasaki, H., 2000. Primary somatosensory cortex is actively involved in pain processing in human. Brain Res. 853 (2), 282–289. doi:10.1016/s0006-8993(99)02274-x.
Karhu, J., Tesche, C.D., 1999. Simultaneous early processing of sensory input in human primary (SI) and secondary (SII) somatosensory cortices. J. Neurophysiol. 81 (5), 2017–2025. doi:10.1152/jn.1999.81.5.2017.
Kasess, C.H., Stephan, K.E., Weissenbacher, A., Pezawas, L., Moser, E., Windischberger, C., 2010. Multi-subject analyses with dynamic causal modeling. Neuroimage 49 (4), 3065–3074. doi:10.1016/j.neuroimage.2009.11.037.
Khoshnejad, M., Piche, M., Saleh, S., Duncan, G., Rainville, P., 2014. Serial processing in primary and secondary somatosensory cortex: a DCM analysis of human fMRI data in response to innocuous and noxious electrical stimulation. Neurosci. Lett. 577, 83–88. doi:10.1016/j.neulet.2014.06.013.
Klingner, C.M., Brodoehl, S., Huonker, R., Gotz, T., Baumann, L., Witte, O.W., 2015. Parallel processing of somatosensory information: evidence from dynamic causal modeling of MEG data. Neuroimage 118, 193–198. doi:10.1016/j.neuroimage.2015.06.028.
Klingner, C.M., Brodoehl, S., Huonker, R., Witte, O.W., 2016. The processing of somatosensory information shifts from an early parallel into a serial processing mode: a combined fMRI/MEG study. Front. Syst. Neurosci. 10, 103. doi:10.3389/fnsys.2016.00103.
Knecht, S., Kunesch, E., Schnitzler, A., 1996. Parallel and serial processing of haptic information in man: effects of parietal lesions on sensorimotor hand function. Neuropsychologia 34 (7), 669–687. doi:10.1016/0028-3932(95)00148-4.
Krubitzer, L.A., Kaas, J.H., 1992. The somatosensory thalamus of monkeys: cortical connections and a redefinition of nuclei in marmosets. J. Comp. Neurol. 319 (1), 123–140. doi:10.1002/cne.903190111.
Li, J., Guido, W., Bickford, M.E., 2003. Two distinct types of corticothalamic EPSPs and their contribution to short-term synaptic plasticity. J. Neurophysiol. 90 (5), 3429–3440. doi:10.1152/jn.00456.2003.
Liang, M., Mouraux, A., Hu, L., Iannetti, G.D., 2013. Primary sensory cortices contain distinguishable spatial patterns of activity for each sense. Nat. Commun. 4. doi:10.1038/ncomms2979, 1979.
Liang, M., Mouraux, A., Iannetti, G.D., 2011. Parallel processing of nociceptive and non-nociceptive somatosensory information in the human primary and secondary somatosensory cortices: evidence from dynamic causal modeling of functional magnetic resonance imaging data. J. Neurosci. 31 (24), 8976–8985. doi:10.1523/JNEUROSCI.6207-10.2011.
Liang, M., Su, Q., Mouraux, A., Iannetti, G.D., 2019. Spatial patterns of brain activity preferentially reflecting transient pain and stimulus intensity. Cereb. Cortex 29 (5), 2211–2227. doi:10.1093/cercor/bhz026.
Liao, C.C., Chen, R.F., Lai, W.S., Lin, R.C., Yen, C.T., 2010. Distribution of large terminal inputs from the primary and secondary somatosensory cortices to the dorsal thalamus in the rodent. J. Comp. Neurol. 518 (13), 2592–2611. doi:10.1002/cne.22354.
Liu, X.B., Honda, C.N., Jones, E.G., 1995. Distribution of four types of synapse on physiologically identified relay neurons in the ventral posterior thalamic nucleus of the cat. J. Comp. Neurol. 352 (1), 69–91. doi:10.1002/cne.903520106.
Mancini, F., Beaumont, A.L., Hu, L., Haggard, P., Iannetti, G.D., 2015. Touch inhibits subcortical and cortical nociceptive responses. Pain 156 (10), 1936–1944. doi:10.1097/j.pain.0000000000000253.
Mima, T., Nagamine, T., Nakamura, K., Shibasaki, H., 1998. Attention modulates both primary and second somatosensory cortical activities in humans: a magnetoencephalographic study. J. Neurophysiol. 80 (4), 2215–2221. doi:10.1152/jn.1998.80.4.2215.
Mo, C., Sherman, S.M., 2019. A sensorimotor pathway via higher-order thalamus. J. Neurosci. 39 (4), 692–704. doi:10.1523/jneurosci.1467-18.2018.
Moeller, S., Yacoub, E., Olman, C.A., Auerbach, E., Strupp, J., Harel, N., Ugurbil, K., 2010. Multiband multislice GE-EPI at 7 tesla, with 16-fold acceleration using partial parallel imaging with application to high spatial and temporal whole-brain fMRI. Magn. Reson. Med. 63 (5), 1144–1153. doi:10.1002/mrm.22361.
Monconduit, L., Lopez-Avila, A., Molat, J.L., Chalus, M., Villanueva, L., 2006. Corticofugal output from the primary somatosensory cortex selectively modulates innocuous and noxious inputs in the rat spinothalamic system. J. Neurosci. 26 (33), 8441–8450. doi:10.1523/jneurosci.1293-06.2006.
Mountcastle, V.B. (2005). The sensory hand: neural mechanisms of somatic sensation.
Mouraux, A., Diukova, A., Lee, M.C., Wise, R.G., Iannetti, G.D., 2011. A multisensory investigation of the functional significance of the "pain matrix". Neuroimage 54 (3), 2237–2249. doi:10.1016/j.neuroimage.2010.09.084.
Murray Sherman, S., Guillery, R.W., 2001. Two types of thalamic relay. In: Murray Sherman, S., Guillery, R.W. (Eds.), Exploring the Thalamus. Academic Press, San Diego, pp. 229–247.
Nichols, T., Brett, M., Andersson, J., Wager, T., Poline, J.B., 2005. Valid conjunction inference with the minimum statistic. Neuroimage 25 (3), 653–660. doi:10.1016/j.neuroimage.2004.12.005.
Nichols, T., Hayasaka, S., 2003. Controlling the familywise error rate in functional neuroimaging: a comparative review. Stat. Methods Med. Res. 12 (5), 419–446. doi:10.1191/0962280203sm341ra.

Niimi, K., Kishi, S., Miki, M., Fujita, S., 1963. An experimental study of the course and termination of the projection fibers from cortical areas 4 and 6 in the cat. Seishin Shinkeigaku Zasshi 17, 167–216. doi:10.1111/j.1440-1819.1963.tb00691.x.

Nothias, F., Peschanski, M., Besson, J.M., 1988. Somatotopic reciprocal connections between the somatosensory cortex and the thalamic Po nucleus in the rat. Brain Res. 447 (1), 169–174. doi:10.1016/0006-8993(88)90980-8.

Oldfield, R.C., 1971. The assessment and analysis of handedness: the Edinburgh inventory. Neuropsychologia 9 (1), 97–113.

Omori, S., Isose, S., Otsuru, N., Nishihara, M., Kuwabara, S., Inui, K., Kakigi, R., 2013. Somatotopic representation of pain in the primary somatosensory cortex (S1) in humans. Clin. Neurophysiol. 124 (7), 1422–1430. doi:10.1016/j.clinph.2013.01.006.

Ploner, M., Schmitz, F., Freund, H.J., Schnitzler, A., 1999. Parallel activation of primary and secondary somatosensory cortices in human pain processing. J. Neurophysiol. 81 (6), 3100–3104. doi:10.1152/jn.1999.81.6.3100.

Ploner, M., Schoffelen, J.M., Schnitzler, A., Gross, J., 2009. Functional integration within the human pain system as revealed by Granger causality. Hum. Brain Mapp. 30 (12), 4025–4032. doi:10.1002/hbm.20826.

Pons, T.P., Garraghty, P.E., Mishkin, M., 1992. Serial and parallel processing of tactual information in somatosensory cortex of rhesus monkeys. J. Neurophysiol. 68 (2), 518–527. doi:10.1152/jn.1992.68.2.518.

Pons, T.P., Kaas, J.H., 1986. Corticocortical connections of area 2 of somatosensory cortex in macaque monkeys: a correlative anatomical and electrophysiological study. J. Comp. Neurol. 248 (3), 313–335. doi:10.1002/cne.902480303.

Power, J.D., Barnes, K.A., Snyder, A.Z., Schlaggar, B.L., Petersen, S.E., 2012. Spurious but systematic correlations in functional connectivity MRI networks arise from subject motion. Neuroimage 59 (3), 2142–2154. doi:10.1016/j.neuroimage.2011.10.018.

Rinvik, E., 1968a. The corticothalamic projection from the pericruciate and coronal gyri in the cat. An experimental study with silver-impregnation methods. Brain Res. 10 (2), 79–119.

Rinvik, E., 1968b. The corticothalamic projection from the second somatosensory cortical area in the cat. An experimental study with silver impregnation methods. Exp. Brain Res. 5 (2), 153–172.

Rowe, M.J., Turman, A.B., Murray, G.M., Zhang, H.Q., 1996. Parallel organization of somatosensory cortical areas I and II for tactile processing. Clin. Exp. Pharmacol. Physiol. 23 (10–11), 931–938. doi:10.1111/j.1440-1681.1996.tb01145.x.

Ruben, J., Schwiemann, J., Deuchert, M., Meyer, R., Krause, T., Curio, G., Villringer, A., 2001. Somatotopic organization of human secondary somatosensory cortex. Cereb. Cortex 11 (5), 463–473. doi:10.1093/cercor/11.5.463.

Sanchez Panchuelo, R.M., Besle, J., Schluppeck, D., Humberstone, M., Francis, S., 2018. Somatotopy in the Human Somatosensory System. Front. Hum. Neurosci. 12, 235. doi:10.3389/fnhum.2018.00235.

Schnitzler, A., Volkmann, J., Enck, P., Frieling, T., Witte, O.W., Freund, H.J., 1999. Different cortical organization of visceral and somatic sensation in humans. Eur. J. Neurosci. 11 (1), 305–315. doi:10.1046/j.1460-9568.1999.00429.x.

Sherman, S.M., 2016. Thalamus plays a central role in ongoing cortical functioning. Nat. Neurosci. 19 (4), 533–541. doi:10.1038/nn.4269.

Shi, T., Stevens, R.T., Tessier, J., Apkarian, A.V., 1993. Spinothalamocortical inputs nonpreferentially innervate the superficial and deep cortical layers of SI. Neurosci. Lett. 160 (2), 209–213. doi:10.1016/0304-3940(93)90415-h.

Spreafico, R., Barbaresi, P., Weinberg, R.J., Rustioni, A., 1987. SII-projecting neurons in the rat thalamus: a single- and double-retrograde-tracing study. Somatosens. Res. 4 (4), 359–375. doi:10.3109/07367228709144614.

Stephan, K.E., Penny, W.D., Daunizeau, J., Moran, R.J., Friston, K.J., 2009. Bayesian model selection for group studies. Neuroimage 46 (4), 1004–1017. doi:10.1016/j.neuroimage.2009.03.025.

Stephan, K.E., Penny, W.D., Moran, R.J., den Ouden, H.E., Daunizeau, J., Friston, K.J., 2010. Ten simple rules for dynamic causal modeling. Neuroimage 49 (4), 3099–3109. doi:10.1016/j.neuroimage.2009.11.015.

Stevens, R.T., London, S.M., Apkarian, A.V., 1993. Spinothalamocortical projections to the secondary somatosensory cortex (SII) in squirrel monkey. Brain Res. 631 (2), 241–246. doi:10.1016/0006-8993(93)91541-y.

Stratford, J., 1954. Cortico-thalamic connections from gyrus proteus and first and second somatic sensory areas of the cat. J. Comp. Neurol. 100 (1), 1–14. doi:10.1002/cne.901000102.

Su, Q., Qin, W., Yang, Q.Q., Yu, C.S., Qian, T.Y., Mouraux, A., . . . Liang, M., 2019. Brain regions preferentially responding to transient and iso-intense painful or tactile stimuli. Neuroimage 192, 52–65. doi:10.1016/j.neuroimage.2019.01.039.

Su, Q., Song, Y., Zhao, R., Liang, M., 2019. A review on the ongoing quest for a pain signature in the human brain. Brain Science Advances 5 (4), 274–287. doi:10.26599/BSA.2019.9050024.

Tauste Campo, A., Vázquez, Y., Álvarez, M., Zainos, A., Rossi-Pool, R., Deco, G., Romo, R., 2019. Feed-forward information and zero-lag synchronization in the sensory thalamocortical circuit are modulated during stimulus perception. Proc. Natl. Acad. Sci. U S A, 116 (15), 7513–7522. doi:10.1073/pnas.1819095116.

Trappenberg, P., 2002. Fundamentals of Computational Neuroscience. Oxford University Press, UK.

Temereanca, S., Simons, D.J., 2004. Functional topography of corticothalamic feedback enhances thalamic spatial response tuning in the somatosensory whisker/barrel system. Neuron 41 (4), 639–651. doi:10.1016/s0896-6273(04)00046-7.

Tracey, I., Mantyh, P.W., 2007. The cerebral signature for pain perception and its modulation. Neuron 55 (3), 377–391. doi:10.1016/j.neuron.2007.07.012.

Treede, R.D., Kenshalo, D.R., Gracely, R.H., Jones, A.K., 1999. The cortical representation of pain. Pain 79 (2–3), 105–111. doi:10.1016/s0304-3959(98)00184-5.

Turman, A.B., Ferrington, D.G., Ghosh, S., Morley, J.W., Rowe, M.J., 1992. Parallel processing of tactile information in the cerebral cortex of the cat: effect of reversible inactivation of SI on responsiveness of SII neurons. J. Neurophysiol. 67 (2), 411–429. doi:10.1152/jn.1992.67.2.411.

Tzourio-Mazoyer, N., Landeau, B., Papathanassiou, D., Crivello, F., Etard, O., Delcroix, N., Joliot, M., 2002. Automated anatomical labeling of activations in SPM using a macroscopic anatomical parcellation of the MNI MRI single-subject brain. Neuroimage 15 (1), 273–289. doi:10.1006/nimg.2001.0978.

Veinante, P., Lavallee, P., Deschenes, M., 2000. Corticothalamic projections from layer 5 of the vibrissal barrel cortex in the rat. J. Comp. Neurol. 424 (2), 197–204. doi:10.1002/1096-9861(20000821)424:2<197::aid-cne1>3.0.co;2-6.

Wager, T.D., Atlas, L.Y., Lindquist, M.A., Roy, M., Woo, C.W., Kross, E., 2013. An fMRI-based neurologic signature of physical pain. N. Engl. J. Med. 368 (15), 1388–1397. doi:10.1056/NEJMoa1204471.

Wang, J.Y., Chang, J.Y., Woodward, D.J., Baccala, L.A., Han, J.S., Luo, F., 2007. Corticofugal influences on thalamic neurons during nociceptive transmission in awake rats. Synapse 61 (5), 335–342. doi:10.1002/syn.20375.

Zeidman, P., Jafarian, A., Corbin, N., Seghier, M.L., Razi, A., Price, C.J., Friston, K.J., 2019a. A guide to group effective connectivity analysis, part 1: first level analysis with DCM for fMRI. Neuroimage 200, 174–190. doi:10.1016/j.neuroimage.2019.06.031.

Zeidman, P., Jafarian, A., Seghier, M.L., Litvak, V., Cagnan, H., Price, C.J., Friston, K.J., 2019b. A guide to group effective connectivity analysis, part 2: second level analysis with PEB. Neuroimage 200, 12–25. doi:10.1016/j.neuroimage.2019.06.032.

Zhang, H.Q., Murray, G.M., Turman, A.B., Mackie, P.D., Coleman, G.T., Rowe, M.J., 1996. Parallel processing in cerebral cortex of the marmoset monkey: effect of reversible SI inactivation on tactile responses in SII. J. Neurophysiol. 76 (6), 3633–3655. doi:10.1152/jn.1996.76.6.3633.

Zhang, H., Sohrabpour, A., Lu, Y., He, B., 2016. Spectral and spatial changes of brain rhythmic activity in response to the sustained thermal pain stimulation. Hum. Brain Mapp. 37 (8), 2976–2991. doi:10.1002/hbm.23220.